Computer simulations in the Gibbs ensemble

by B. SMIT and PH. DE SMEDT

Koninklijke/Shell-Laboratorium, Amsterdam, (Shell Research B.V.),
Badhuisweg 3, 1031 CM Amsterdam, The Netherlands

and D. FRENKEL

FOM Institute for Atomic and Molecular Physics,
Kruislaan 407, 1098 SJ Amsterdam, The Netherlands

In this article we demonstrate that the Gibbs ensemble and the canonical ensemble are equivalent in the thermodynamic limit. Furthermore, we discuss some interesting aspects of the method when applied close to the critical point. We show that for a finite number of particles the Gibbs ensemble leads to a lower value of the critical temperature of the finite system than that obtained by standard N,V,T simulations with the same number of particles. This is due to entropic considerations. Simulations in the Gibbs ensemble, because it allows for fluctuations in the number of particles and in the volume of the sub-systems, may lead to a better estimate of the critical temperature of the infinite system.

1. Introduction

Until recently it was an enormous task to obtain a vapour–liquid coexistence curve for a model fluid using computer simulation techniques. The conventional methods require many simulations along an isotherm. For each state point the pressure is calculated and the chemical potential is obtained by thermodynamic integration or by test particle methods [1]. The densities of the coexisting liquid and vapour phases at a given temperature are obtained indirectly by equating the pressure and the chemical potential.

The number of particles in a simulation is limited by the available computer time. When a system is simulated containing a liquid in coexistence with a vapour, the interface between the gas and liquid phase will dominate the properties of the system and therefore influence the bulk properties, if the number of particles is small. In order to eliminate these surface effects one has to simulate a very large number of particles or adopt the cumbersome route outlined above.

A new simulation technique proposed by Panagiotopoulos [2, 3], which samples the Gibbs ensemble, enables vapour–liquid coexistence to be simulated without the presence of an interface. Therefore, data on vapour–liquid equilibria can be obtained with a relatively small number of particles via a single simulation.

In his original article Panagiotopoulos [2] introduced the Gibbs ensemble and derived the acceptance rules using fluctuation theory. In this article we demonstrate more formally that the Gibbs ensemble and the canonical ensemble are equivalent in the thermodynamic limit by considering the free energy density in the Gibbs ensemble. In this respect it is important to note that Panagiotopoulos [2] used this method successfully to study the vapour–liquid coexistence curve of the Lennard-

Jones fluids. The excellent agreement of his results with the results obtained by ordinary simulations is in itself strong evidence that simulations in the Gibbs ensemble yield reliable results.

However, our arguments also reveal some unexpected interesting facts concerning the method when it is applied close to the critical point. Indeed, a careful analysis of the surface contributions to this free energy density reveals that close to, but below the critical temperature of the *finite system*, no vapour–liquid coexistence can be observed. These theoretical observations are confirmed by the results of computer simulations. However, since simulations for a N,V,T system overestimate the value of the critical temperature, the Gibbs ensemble may in fact lead to a better estimate for the critical temperature of the infinite system.

In the following sections we first prove the equivalence of the Gibbs ensemble and the canonical ensemble in the thermodynamic limit. We then consider the free energy density for a finite system and discuss the consequence for actual simulations.

2. The free energy in the Gibbs ensemble

In this section we show that the free energy for the Gibbs ensemble, when correctly defined, equals the free energy of the canonical ensemble. Before we proceed, we first list a few basic results for the free energy in the canonical ensemble.

2.1. *Basic definitions and results*

Consider a system of N particles in a volume V and temperature T (canonical ensemble). The partition function is defined as (see Ruelle [4])

$$Z_{N, V, T} \equiv \frac{1}{\Lambda^{3N} N!} \int_V dr_1, \ldots, dr_N \exp \left[-\beta U(r_1, \ldots, r_N) \right] \qquad (1)$$

where Λ is the thermal de Broglie wavelength and r the coordinates of the particles. The free energy density is defined in the thermodynamic limit by

$$f(\rho) \equiv \lim_{V \to \infty} f_V(\rho) \equiv \lim_{\substack{V \to \infty \\ N/V = \rho}} -\frac{1}{\beta V} \log Z_{N, V, T}, \qquad (2)$$

or

$$Z_{N, V, T} = \exp \left[-\beta V \left(f(\rho) + o\left(\frac{1}{V}\right) \right) \right]. \qquad (3)$$

It can be shown that this free energy is a convex function of the density ρ [4]:

$$f(x\rho_1 + (1 - x)\rho_2) \leqslant x f(\rho_1) + (1 - x) f(\rho_2), \qquad (4)$$

for every ρ_1, ρ_2 and $0 < x < 1$. The equality holds in the case of a first order transition, if $\rho_g \leqslant \rho_1 \leqslant \rho_2 \leqslant \rho_1$, where ρ_g, ρ_1 denote the density of coexisting gas and liquid phases respectively.

Another interesting result is the well-known saddle point theorem [5] (also called the steepest descent method). We state the results in the following form.

Assume that $Z_{N, V, T}$ can be written as

$$Z_{N, V, T} \equiv \int dx_1, \ldots, dx_m \exp \left[-\beta V \left(f_m(x_1, \ldots, x_m) + o\left(\frac{1}{V}\right) \right) \right] \qquad (5)$$

and define

$$f(\rho) \equiv \min_{x_1, \ldots, x_m} f_m(x_1, \ldots, x_m). \qquad (6)$$

Assume that $f_m(x_1, \ldots, x_m)$ and the term $o(1/V)$ satisfy a few technical conditions, which hold for most statistical mechanics systems [5]. Then

$$\lim_{\substack{V \to \infty \\ N/V = \rho}} -\frac{1}{\beta V} \log Z_{N, V, T} = f(\rho). \qquad (7)$$

Moreover, define

$$\langle F(x_1, \ldots, x_m) \rangle_V$$

$$= \frac{\int dx_1, \ldots, dx_m \, F(x_1, \ldots, x_m) \exp \left[-\beta V (f(x_1, \ldots, x_m) + o\left(\frac{1}{V}\right)) \right]}{Z_{N, V, T}}. \qquad (8)$$

Then a function $G(x_1, \ldots, x_m) \geqslant 0$ exists with support on the surface S

$$S = \{ y_1, \ldots, y_m \,|\, f_m(y_1, \ldots, y_m) = \min_{x_1, \ldots, x_m} f_m(x_1, \ldots, x_m) \} \qquad (9)$$

and normalization

$$\int_S dx_1, \ldots, dx_m \, G(x_1, \ldots, x_m) = 1$$

such that, for an arbitrary function F

$$\langle F(x_1, \ldots, x_m) \rangle \equiv \lim_{V \to \infty} \langle F(x_1, \ldots, x_m) \rangle_V$$

$$= \int_S dx_1, \ldots, dx_m \, G(x_1, \ldots, x_m) F(x_1, \ldots, x_m). \qquad (10)$$

We are now ready to start the main part of this section.

2.2. *The free energy density in the Gibbs ensemble*

The Gibbs ensemble can be defined by introducing a system of N particles in a constant (total) volume V and at a constant temperature (T). This system is divided into two (separate) sub-systems labelled 1 and 2. The (variable) volumes of these sub-systems are V_1 and V_2 and (variable) number of particles N_1 and N_2 respectively. Note that $V = V_1 + V_2$ and $N = N_1 + N_2$. The partition function for the Gibbs ensemble is given by [6]

$$\bar{Z}_{N, V, T} = \frac{1}{\Lambda^{3N} N!} \sum_{N_1 = 0}^{N} \frac{N!}{N_1! N_2!} \int_0^V dV_1 \int_{V_1} dr_1, \ldots, dr_{N_1} \int_{V_2} dr_{N_1+1}, \ldots, dr_N$$

$$\times \exp \left[-\beta (U(r_1, \ldots, r_{N_1}) + U(r_{N_1+1}, \ldots, r_N)) \right]. \qquad (11)$$

Note that this expression is almost equal to the expression for the canonical ensemble

$$Z_{N, V, T} = \frac{1}{\Lambda^{3N} N!} \sum_{N_1=0}^{N} \frac{N!}{N_1! N_2!} \int_0^V dV_1 \int_{V_1} dr_1, \ldots, dr_{N_1} \int_{V_2} dr_{N_1+1}, \ldots, dr_N$$

$$\times \exp\left[-\beta(U(r_1, \ldots, r_{N_1}) + U(r_{N_1+1}, \ldots, r_N)\right.$$

$$\left. + \text{ interactions between the two volumes})\right]. \qquad (12)$$

In the case of short-range interactions, the last term in the exponent of equation (12) is proportional to a surface term. This already suggests that both ensembles should behave similarly in many respects. We work out these ideas more rigorously in the following pages.

In the usual way, we define as a free energy in the Gibbs ensemble

$$\bar{f}(\rho) \equiv \lim_{\substack{V \to \infty \\ N/V = \rho}} -\frac{1}{\beta V} \log \bar{Z}_{N, V, T}. \qquad (13)$$

Now $\bar{Z}_{N, V, T}$ can be written as

$$\bar{Z}_{N, V, T} = \sum_{N_1=0}^{N} \int_0^V dV_1 Z_{N_1, V_1, T} Z_{N-N_1, V-V_1, T}, \qquad (14)$$

where $Z_{N, V, T}$ is as in equation (1). Introducing $x = N_1/N$ and $y = V_1/V$, and assuming that the number of particles is very large, we can then write

$$\bar{Z}_{N, V, T} = NV \int_0^1 dx \int_0^1 dy \bar{Z}_N(x, y), \qquad (15)$$

where

$$\bar{Z}_N(x, y) = Z_{xN, yV, T} Z_{(1-x)N, (1-y)V, T}$$

$$= \exp\left[-\beta V \left\{ yf\left(\frac{x}{y}\rho\right) + (1-y)f\left(\frac{1-x}{1-y}\rho\right) + o\left(\frac{1}{V}\right) \right\} \right]. \qquad (16)$$

To obtain the free energy density $\bar{f}(\rho)$, we can now apply the saddle point theorem (equation (7))

$$\bar{f}(\rho) = \min_{\substack{0 \leqslant x \leqslant 1 \\ 0 \leqslant y \leqslant 1}} \left\{ yf\left(\frac{x}{y}\rho\right) + (1-y)f\left(\frac{1-x}{1-y}\rho\right) \right\} \equiv \min_{\substack{0 \leqslant x \leqslant 1 \\ 0 \leqslant y \leqslant 1}} \{\bar{f}(x, y)\}. \qquad (17)$$

We now have to find the surface S on which the function $\bar{f}(x, y)$ reaches its minimum. Application of equation (4) yields

$$\bar{f}(x, y) \geqslant f\left(y \frac{x}{y}\rho + (1-y)\frac{1-x}{1-y}\rho\right) = f(\rho). \qquad (18)$$

We first consider the case where there is only one phase. In this case the equality in equation (18) holds only if

$$\frac{x}{y}\rho = \frac{1-x}{1-y}\rho = \rho, \qquad \text{or} \quad x = y. \qquad (19)$$

Thus for a single phase S is given by

$$S = \{(x, y) \mid x = y\}. \tag{20}$$

Secondly, we consider the case of a first order phase transition. Let ρ be such that $\rho_l \leqslant \rho \leqslant \rho_g$, and let us choose x and y such that

$$\rho_g \leqslant \frac{x}{y} \rho \equiv \rho_3 \leqslant \rho_l \quad \text{and} \quad \rho_g \leqslant \frac{(1 - x)}{(1 - y)} \rho \equiv \rho_4 \leqslant \rho_l. \tag{21}$$

Using equation (4), we can write for $\bar{f}(x, y)$

$$\bar{f}(x, y) = y f(\rho_3) + (1 - y) f(\rho_4),$$
$$= f(y \rho_3) + f((1 - y)\rho_4). \tag{22}$$

Note that

$$(y\rho_3 + (1 - y)\rho_4) = \rho, \tag{23}$$

which gives

$$\bar{f}(x, y) = f(\rho). \tag{24}$$

It can be shown that, if x, y do not satisfy equation (21), $\bar{f}(x, y) > f(\rho)$.

Therefore the surface S in case of a first order phase transition is given by:

$$S = \left\{(x, y) \mid \rho_g \leqslant \frac{x}{y} \rho \leqslant \rho_l, \rho_g \leqslant \frac{(1 - x)}{(1 - y)} \rho \leqslant \rho_l \right\}. \tag{25}$$

Thus we have shown that in the thermodynamic limit the free energy of the Gibbs ensemble is equal to the free energy of the canonical ensemble. Furthermore we have determined the surface S where $\bar{f}(x, y)$ reaches its minimum.

It remains to determine the function $G(x, y)$. In case of a pure phase $G(x, y)$ needs to be of the form

$$G(x, y) = g(x)\delta(x - y). \tag{26}$$

It is shown in Appendix 1 that for the free gas $g(x) = 1$. We expect that the same holds for an interacting gas. Evidence is given in figure 1, which shows a probability plot in the x, y plane for a simulation of a finite system at high temperature.

In the case of two phases we will prove that $G(x, y)$ is given by

$$G(x, y) = \tfrac{1}{2}\delta\left(x - \frac{\rho_g}{\rho}\frac{\rho - \rho_g}{\rho_l - \rho_g}\right)\delta\left(y - \frac{\rho - \rho_g}{\rho_l - \rho_g}\right)$$
$$+ \tfrac{1}{2}\delta\left(x - \frac{\rho_l}{\rho}\frac{\rho_l - \rho}{\rho_l - \rho_g}\right)\delta\left(y - \frac{\rho_l - \rho}{\rho_l - \rho_g}\right). \tag{27}$$

This equation indicates that the system will split up into a liquid phase with density ρ_l and a vapour phase with density ρ_g.

To show the previous result, we take into account the next significant term in the expression for the free energy (equation (3)), which is the term due to the surface tension. This term will be present when phase separation occurs in our box. Taking into account this surface term we get for the partition function

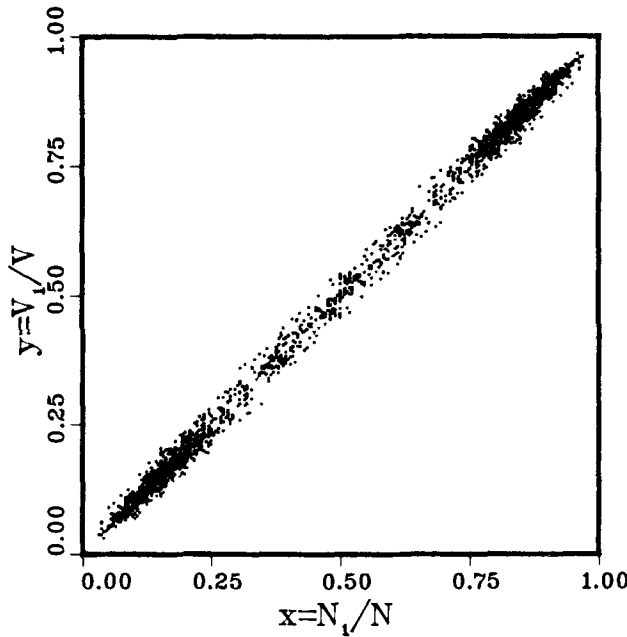$$Z_{N, V, T} = \exp\left[-\beta(V f(\rho) + \gamma A + o(A))\right], \tag{28}$$

Figure 1. Probability plot in the x, y plane ($x = N_1/N$, $y = V_1/V$) for a Lennard-Jones fluid
at $T^* = 5\cdot21$ ($N = 216$ and $V = 670$). The total number of cycles in this simulation
was 6000 (see Appendix 2). After 6 cycles the points (x_i, y_i) and ($1 - x_i, 1 - y_i$) were
plotted in the x, y plane.

where A denotes the area of the interface and γ denotes the interfacial tension. This
area will in general be proportional to $V^{2/3}$. Using this form of the partition func-
tion for the Gibbs ensemble, equation (8) can be written as

$$\langle F(x, y)\rangle_V = \frac{\displaystyle\iint dx\,dy F(x, y) \exp\left[-\beta(Vf(x, y) + \gamma V^{2/3}a(x, y) + o(V^{2/3}))\right]}{Z_{N, V, T}}, \quad (29)$$

where $a(x, y)$ is a function of the order of unity.

We know from the saddle point theorem that the most important contribution
to the integrals comes from the region S, defined by equation (25). Thus

$$\langle F(x, y)\rangle_V \simeq \frac{\displaystyle\iint_S dx\,dy F(x, y) \exp\left[-\beta(Vf(x, y) + \gamma V^{2/3}a(x, y) + o(V^{2/3}))\right]}{\displaystyle\iint_S dx\,dy \exp\left[-\beta(Vf(x, y) + \gamma V^{2/3}a(x, y) + o(V^{2/3}))\right]} \quad (30)$$

and applying the saddle point theorem again yields

$$\langle F(x, y)\rangle_V \simeq \frac{\displaystyle\iint_{S_A} dx\,dy F(x, y) \exp\left[-\beta\gamma V^{2/3}a(x, y) + o(V^{2/3})\right]}{\displaystyle\iint_{S_A} dx\,dy \exp\left[-\beta\gamma V^{2/3}a(x, y) + o(V^{2/3})\right]} \quad (31)$$

$$\lim_{V \to \infty} \langle F(x, y)\rangle_V = \iint_{S_A} dx\,dy G(x, y)F(x, y) \quad (32)$$

where the surface S_A is now given by

$$S_A = \left\{ (x, y) \mid a(x, y) = \min_{\bar{x}, \bar{y}} a(\bar{x}, \bar{y}) \right\}. \tag{33}$$

In the infinite system the area of the interface is zero if box 1 contains only gas (liquid) and box 2 only liquid (gas). Therefore S_A is given by

$$S_A = \left\{ (x, y) \mid \frac{x}{y} = \rho_l \quad \text{and} \quad \frac{1-x}{1-y} = \rho_g \quad \text{or} \quad \frac{x}{y} = \rho_g \quad \text{and} \quad \frac{1-x}{1-y} = \rho_l \right\}. \tag{34}$$

It is straightforward to show that this surface results in expression (27) for $G(x, y)$.

Summarizing, we have shown that the free energy density for the Gibbs ensemble, as defined by equation (13), becomes identical to the free energy density of the canonical ensemble. Furthermore, it is shown that, at high temperatures, $x = y$, i.e. the densities in the two sub-systems of the Gibbs ensemble are equal and equal to the density in the canonical ensemble (see figure 1).

In the case of a first order phase transition, if surface terms would be unimportant x and y are restricted to the area defined by (cf. equation (25))

$$\rho_g \leqslant \frac{x}{y} \rho \equiv \rho_3 \leqslant \rho_l \quad \text{and} \quad \rho_g \leqslant \frac{(1-x)}{(1-y)} \rho \equiv \rho_4 \leqslant \rho_l. \tag{35}$$

If we take surface effects into account it is shown that this surface (equation (35)) reduces to two points in the x, y plane. The densities of these points correspond to the density of the gas or liquid phase in the canonical ensemble.
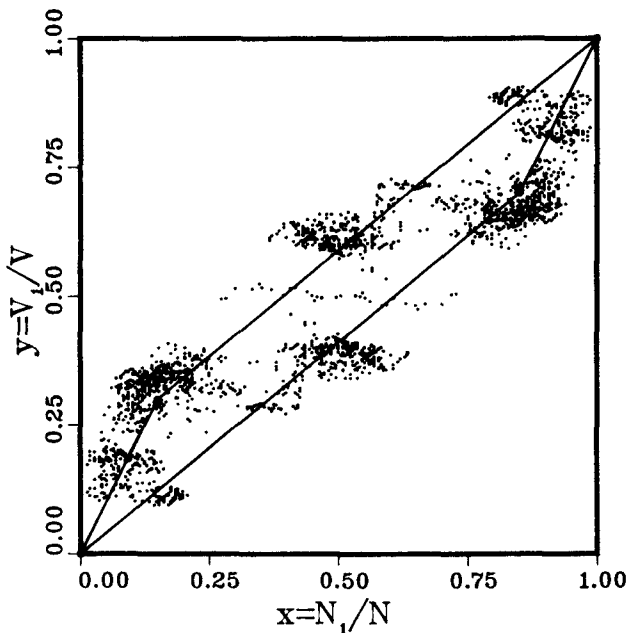

Figure 2. Probability plot in the x, y plane ($x = N_1/N$, $y = V_1/V$) for a Lennard-Jones fluid slightly below the critical temperature ($T^* = 1\cdot30$, $N = 512$ and $V = 1600$). The solid lines show the area S as defined in equation 35 and the two large dots the (x, y) corresponding to the coexisting gas and liquid phase; see also the caption to figure 1.
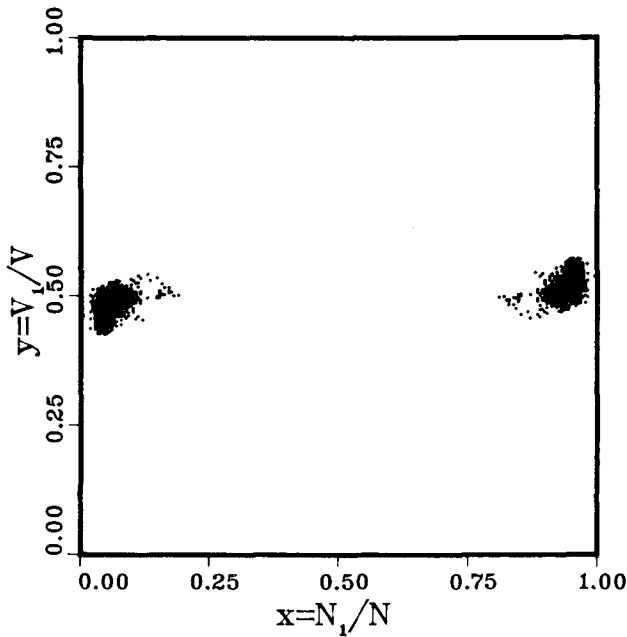
Figure 3.   Probability plot in the x, y plane ($x = N_1/N$, $y = V_1/V$) for a Lennard-Jones fluid well below the critical temperature ($T^* = 1\cdot15$, $N = 216$ and $V = 670$), see also the caption to figure 1.

It is interesting to compare this with the results of an actual simulation of a finite system. In Figure 3 the results for a simulation at a temperature well below the critical point are given. This shows that the surface reduces to two points. This should be compared to the results of a simulation close to the critical point (figure 2). At those conditions the interfacial tension is very small and we see that the simulation samples the entire surface S. Note that due to the finite size of this system fluctuations are also possible in which the density of a sub-system becomes greater/smaller than the density of the liquid/gas phase.

In the next section we will study in more detail the consequences of these results for simulations of a finite number of particles.

3.   Surface contributions to the free energy for finite systems in the Gibbs ensemble

For the infinite system we have shown that in case of a first order phase transition one of the sub-systems will contain the gas (liquid) phase and the other sub-system will contain the liquid (gas) phase. For a finite system we have to calculate the surface area for a given x, y ($= V^{2/3}a(x, y)$) and the surface contribution of the free energy can be obtained from

$$F_{surf}(x, y) = V^{2/3}\gamma a(x, y). \tag{36}$$

In order to calculate $a(x, y)$ we have to find that form of the interface which has a minimal surface area. If we perform a simulation with the normal periodic boundary conditions, we can distinguish between a drop of liquid, a drop of gas and a

Droplet of gas in liquid   Droplet of liquid in gas   Double layer
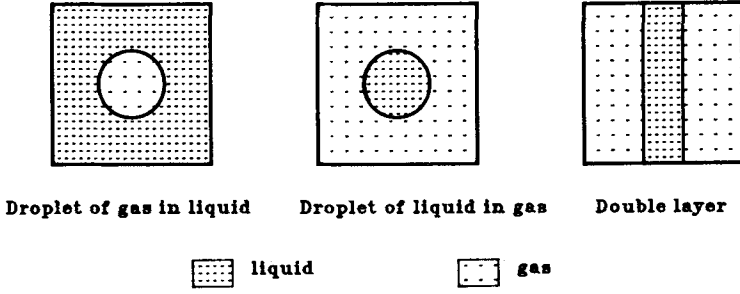
liquid   gas

Figure 4. Schematic representation of one of the boxes in a Monte Carlo simulation in the Gibbs ensemble slightly below the critical temperature.

double layer (see figure 4). The area of a sphere with volume V_{drop} is given by

$$A_S = 4\pi \left(\frac{3}{4\pi} V_{\text{drop}} \right)^{2/3} \tag{37}$$

while the area of a double layer in a cubic box with volume V_{box} is given by

$$A_{\text{DI}} = 2(V_{\text{box}})^{2/3}. \tag{38}$$

A straightforward calculation yields the following expression for the volume of liquid in sub-volume 1 (V_1^1), the volume of gas in sub-volume 1 (V_g^1), the volume of liquid in sub-volume 2 (V_1^2), and the volume of gas in sub-volume 2 (V_g^2)

$$V_1^1 = y \frac{\rho_1 - \dfrac{x}{y} \rho}{\rho_1 - \rho_g} V \equiv y f_1^1 V, \tag{39}$$

$$V_g^1 = y \frac{\dfrac{x}{y} \rho - \rho_g}{\rho_1 - \rho_g} V \equiv y f_g^1 V, \tag{40}$$

$$V_1^2 = (1 - y) \frac{\rho_1 - \dfrac{(1 - x)}{(1 - y)} \rho}{\rho_1 - \rho_g} V \equiv (1 - y) f_1^2 V, \tag{41}$$

$$V_g^2 = y \frac{\dfrac{(1 - x)}{(1 - y)} \rho - \rho_g}{\rho_1 - \rho_g} V \equiv (1 - y) f_g^2 V, \tag{42}$$

where f_g^1 denotes the volume fraction of gas in sub-volume 1. Combining these results we obtain the following expression for the surface contribution to the free energy

$$a(x, y) = \{ y^{2/3} \min (a_1^1, a_g^1, a_{\text{DI}}^1) + (1 - y)^{2/3} \min (a_1^2, a_g^2, a_{\text{DI}}^2) \} \tag{43}$$

where

$$a_{g, 1}^i = 4\pi \left(\frac{3}{4\pi} f_{g, 1}^i \right)^{2/3} \tag{44}$$
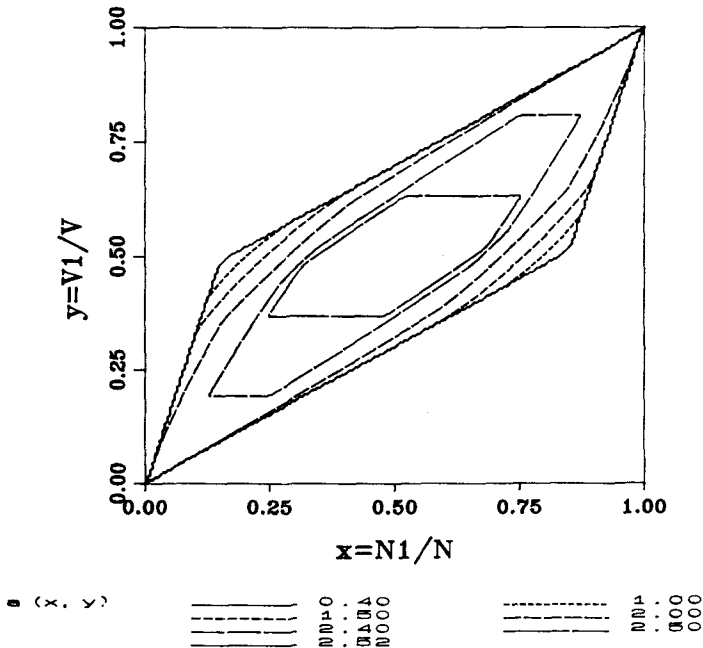
$$a_{\text{DI}}^i = 2. \tag{45}$$

Figure 5.   Contour plot in the x, y plane ($x = N_1/N$, $y = V_1/V$) of the surface contribution ($a(x, y)$) to the free energy of the Gibbs ensemble (equation (25)). Note that the x, y values of the coexisting vapour and liquid phase are chosen arbitrarily.

In figure 5 we have plotted the function $a(x, y)$ on the x, y plane. This plot shows that there are two minima, which corresponds to the case where there is only vapour or liquid in the sub-systems. Furthermore, it shows that there are large parts in the x, y plane where the gradient is very small. In figure 6 we have plotted the results of a simulation close to the critical point. From this plot we observe that a large area in the x, y plane is sampled which is far from the desired results. These fluctuations are not so obvious when the density probability function is considered (figure 7(a)), but the average gas and liquid densities might be influenced quite substantially. Therefore it is important to check for consistency of the results by plotting a probability density in the x, y plane. Because the gradients towards the global minima are very small (cf. figure 5), it is possible for a simulation to become trapped in those areas.

Another simple indication of a drift in the x, y plane can be obtained from a probability distribution of the volumes. At a given temperature the densities of the coexisting phases are given (but unknown) and because the total number of particles and total volume remain fixed, the probability function of the volume must have two (sharp) peaks if the simulation samples the x, y plane correctly (see figures 7 and 8). If this probability function does not give two sharp peaks it is likely that the simulation is trapped in such a region (compare figures 3 and 6).

It is interesting to calculate the probability of finding the density ρ in one of the sub-volumes for a finite system. This should roughly be given by:

$$P(\rho) = \frac{\iint_S dx\, dy\, \delta(x - y\rho) \exp\left[-\beta F_{\mathrm{surf}}(x, y)\right]}{\iint_S dx\, dy \exp\left[-\beta F_{\mathrm{surf}}(x, y)\right]}. \tag{46}$$
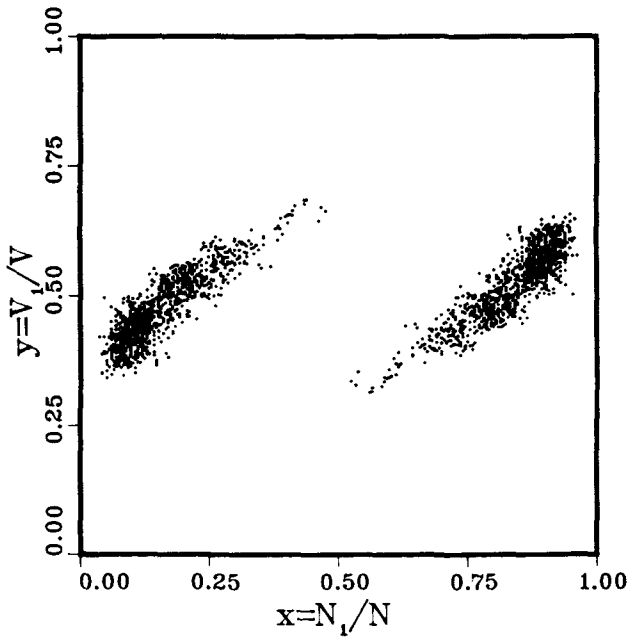
Figure 6. Probability plot in the x, y plane ($x = N_1/N$, $y = V_1/V$) for a Lennard-Jones fluid below the critical temperature ($T^* = 1 \cdot 20$ and $N = 216$). Due to an unfortunate fluctuation the system became trapped in a local minimum (compare figure 5); see also the caption to figure 1.

In order to study the temperature dependence we have assumed that close to the critical temperature the interfacial tension depends on the temperature according to [7]:

$$\gamma = \gamma_0 \left(1 - \frac{T}{T_c} \right)^\mu, \tag{47}$$

where $\mu = 1 \cdot 26$ (critical exponent [7]). Furthermore, in order to calculate the area S, which is defined by the densities of the coexisting gas and liquid phases at the given temperature (equation (25)), we have fitted the result of Panagiotopoulos [2] to the scaling law for the densities [7].

When the system is infinite, we have shown (combine equations (27, 32 and 46))

$$P(\rho) = \tfrac{1}{2}\delta(\rho - \rho_g) + \tfrac{1}{2}\delta(\rho - \rho_l). \tag{48}$$

However, for a finite system this function has interesting behaviour. In figures 9 (*a–c*) we have plotted $P(\rho)$ for a Lennard-Jones fluid ($\gamma_0 = 2 \cdot 71$ [7] and $T_c = 1 \cdot 32$ [2]) for 64, 216 and 512 particles respectively. These figures demonstrate that as the temperature is increased the following transitions can be observed. Since at low temperature the surface tension is large, it is unlikely that vapour and liquid will coexist is the same sub-volume. Therefore, at low temperature there are two sharp peaks, which correspond to the two coexisting phases. As the temperature increases, the surface tension decreases and becomes comparable to the entropy associated with the formation of an interface (there are simply more densities where vapour and liquid can coexist). Note that around $x = y$ the interface will be a double layer and therefore small deviations around this line do not change the surface free energy
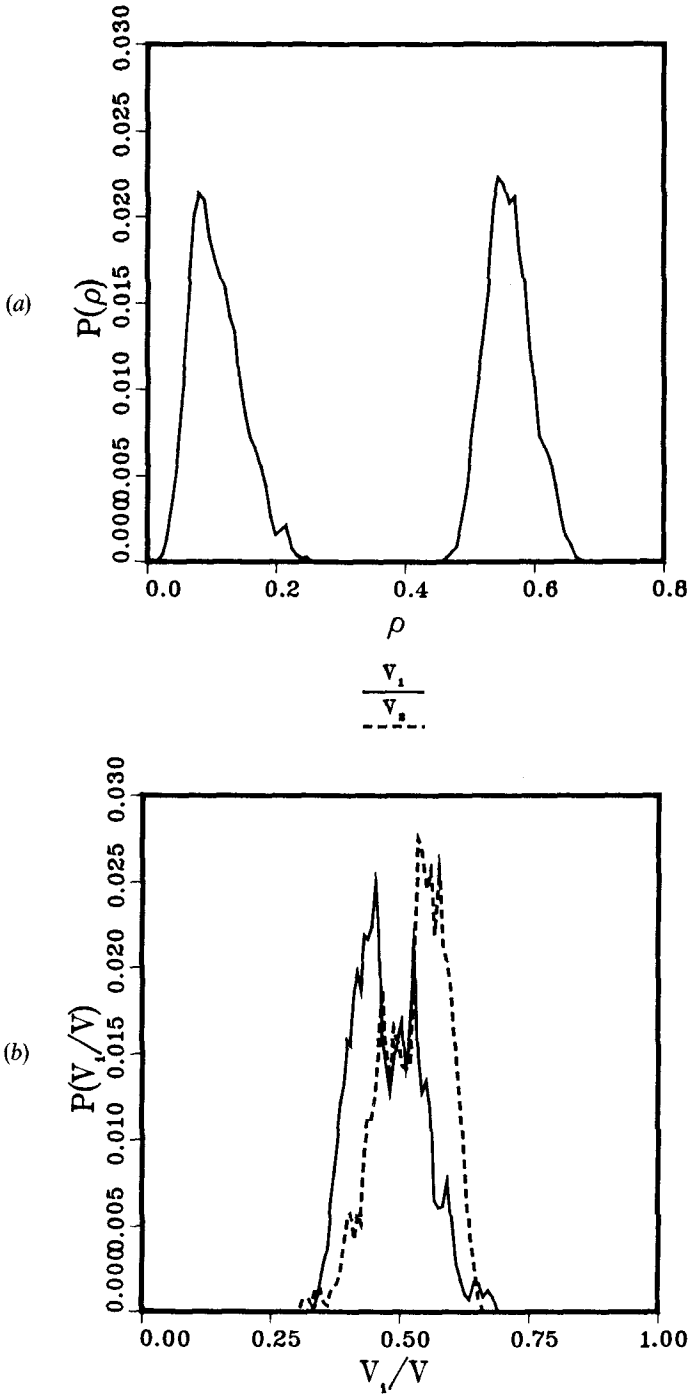
Figure 7.   Density probability function (*a*) and volume probability function (*b*) for a
    Lennard-Jones fluid below the critical temperature ($T^* = 1.20$ and $N = 216$). These
    probability functions were obtained by calculating each cycle the volumes of the
    sub-systems and densities in both sub-systems and updating a histogram. At the end of
    the simulations these histograms were divided by the total number of cycles (see also
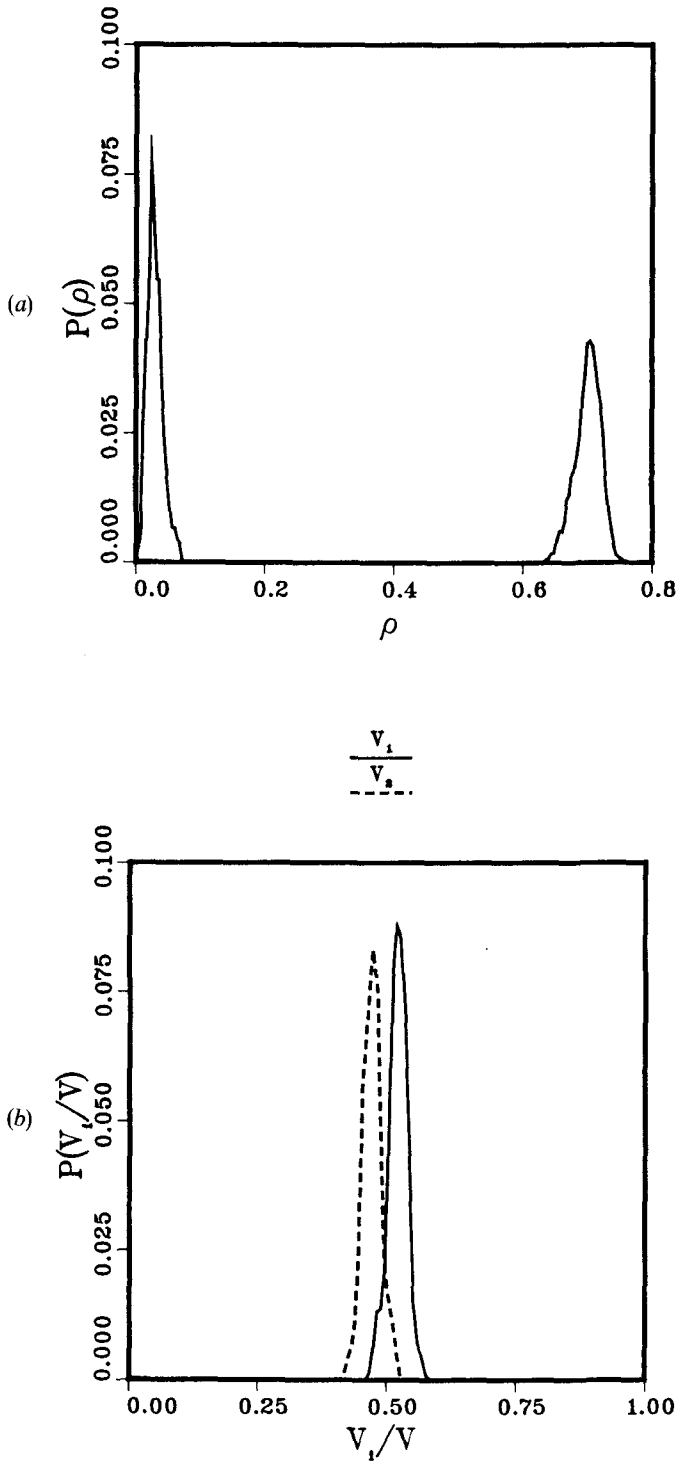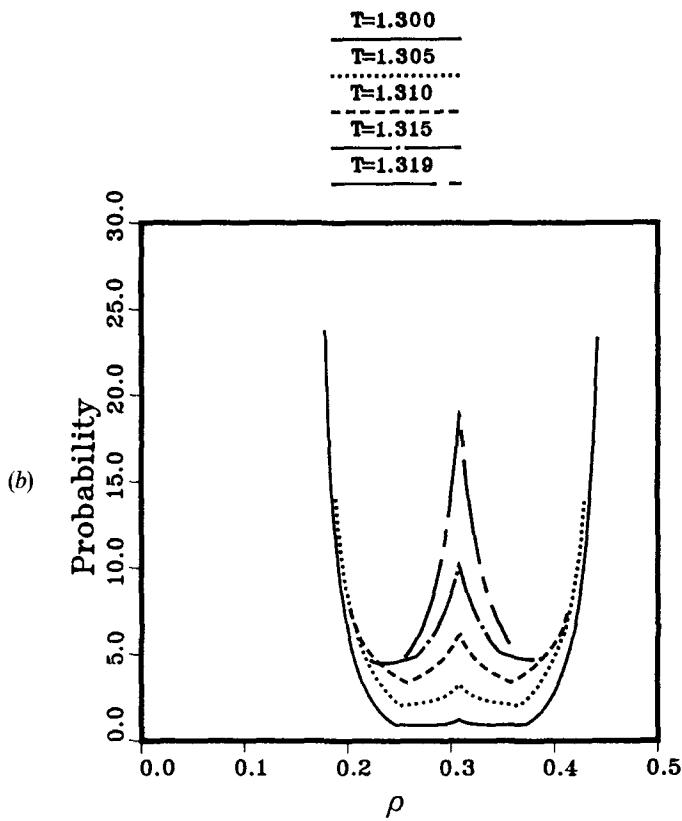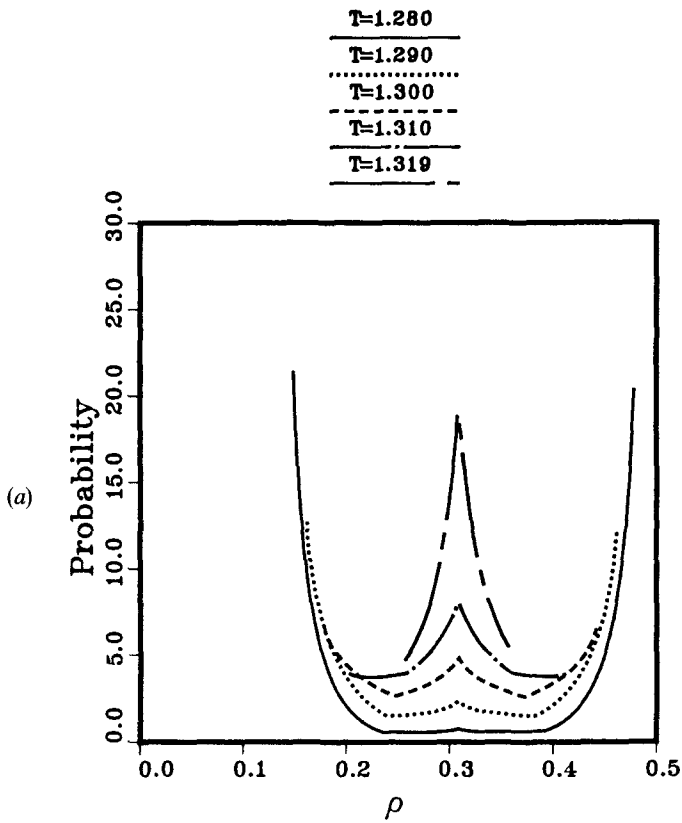   Appendix 2).

Figure 8. Density probability function (*a*) and volume probability function (*b*) for a Lennard-Jones fluid well below the critical temperature ($T^* = 1\cdot15$ and $N = 216$); see also the caption to figure 7.
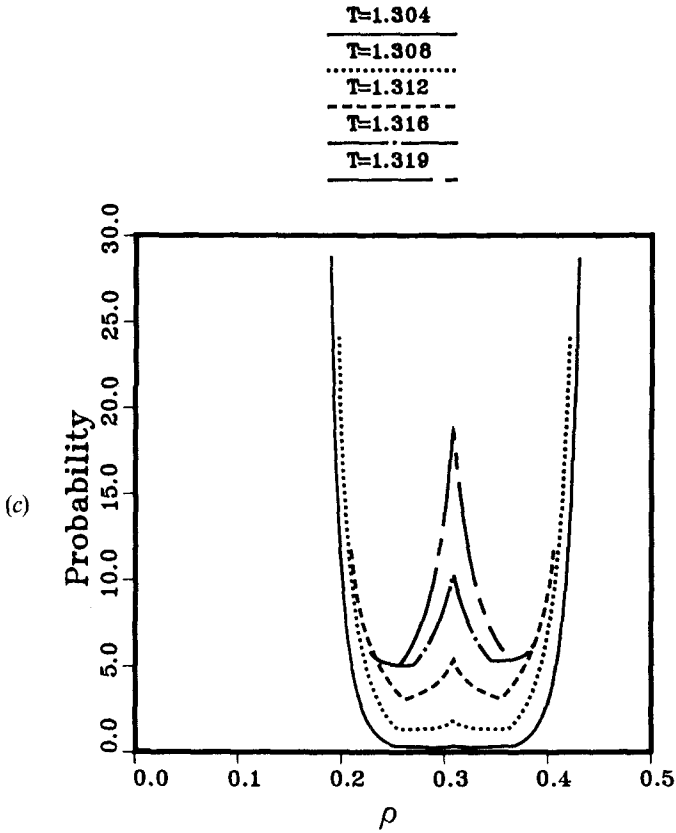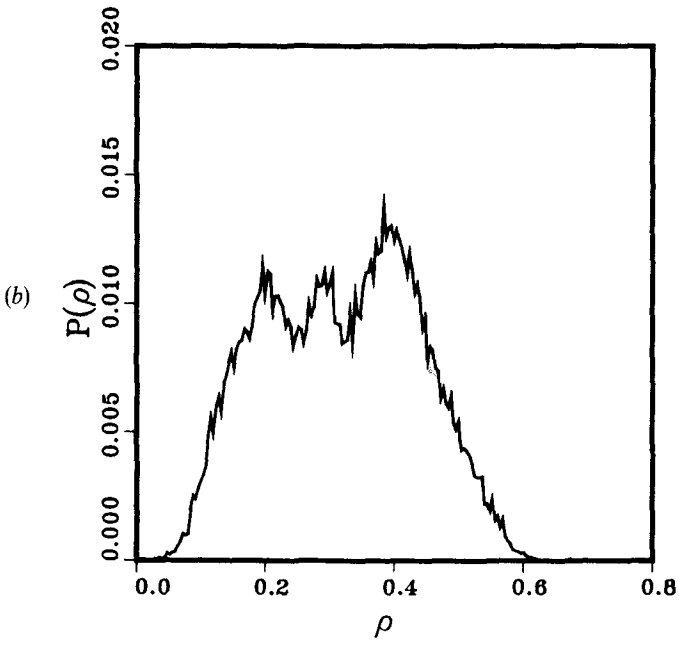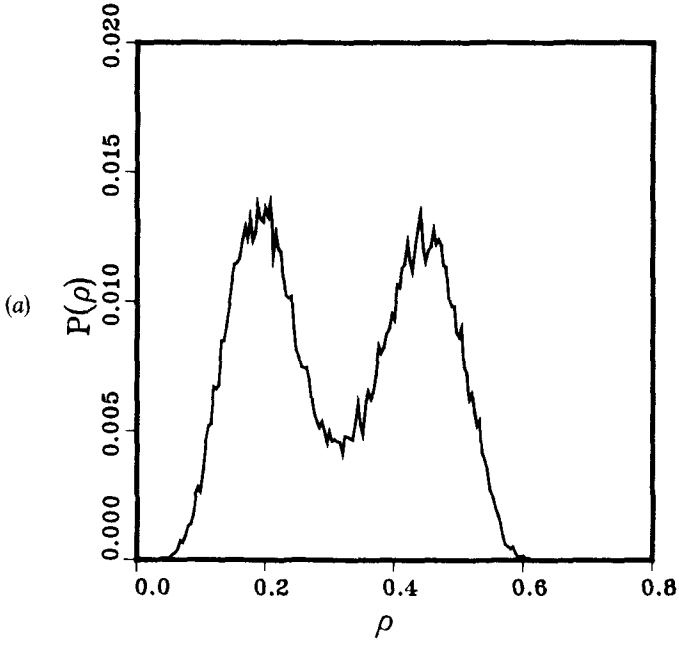
Figure 9.   Calculated density probability functions (equation (47)) at different temperatures for various numbers of particles (*a*) $N = 64$, (*b*) $N = 216$ and (*c*) $N = 512$. Note that in each figure the temperatures are different and that the curves are drawn for $\rho_g(T) < \rho < \rho_l(T)$.

contribution (see figures 4 and 5). Furthermore, $x = y$ is the longest 'strip' in the x, y plane on the surface S. These entropic considerations explain the appearance of the third peak at the average density ρ. When the temperature is increased further this entropy effect will dominate the surface contribution and the peaks of the coexisting phases will disappear close to, but below, the critical temperature of the finite system.

Note that the temperature range over which these transitions occur depends on the number of particles. Comparison with the results for 64 particles (figure 9(*a*)) shows that the third peak exists over a larger temperature range.

It is interesting to compare these results with probability distributions for the densities obtained from simulations for the Lennard-Jones fluid. In figure 10(*a*, *b*, *c*) the results are presented for simulations with 216 particles at $T^* = 1.30$ (*a*), $T^* = 1.31$ (*b*) and $T^* = 1.315$ (*c*). Comparison with the theoretical results (figure 9(*b*)) shows not only that the transitions from two peaks at low temperatures to three peaks and finally to one peak below the critical temperature are observed but also that the temperature range of these transitions is in good agreement with the theoretical predictions.
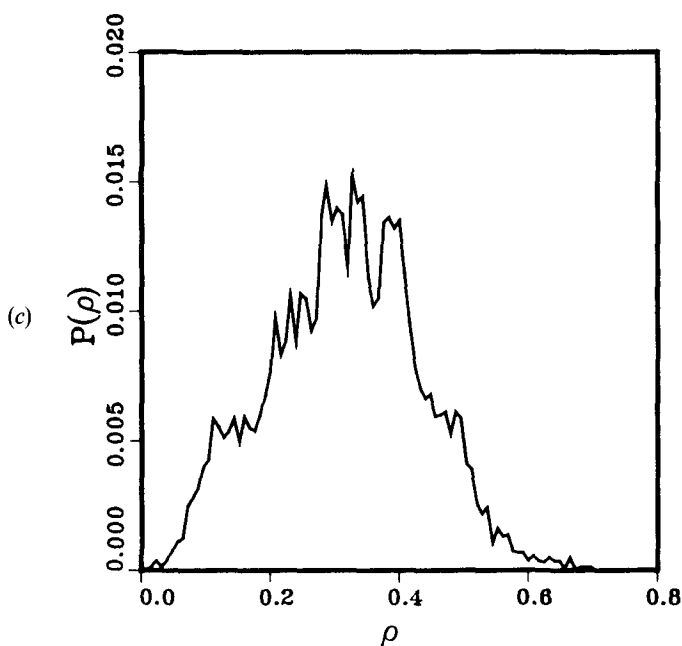
Figure 10.   Density probability functions for a Lennard-Jones fluid as obtained from simulations ($N = 216$) at various temperatures: (*a*) $T^* = 1\cdot30$, (*b*) $T^* = 1\cdot31$ and (*c*) $T^* = 1\cdot315$; see also the caption to figure 7.

4.   Concluding remarks

In this article we have demonstrated that the Gibbs ensemble and the canonical ensemble yield equivalent results in the thermodynamic limit. Furthermore, for a finite system sufficiently far from the critical point, where the interfacial tension between the liquid and gas phase is high, we have found that the Gibbs ensemble gives reliable estimates of the densities of the coexisting liquid and gas phases.

We have further found that close to, but below the critical temperature of the finite system, the sub-systems will not yet be found in the liquid phase or the gas phase, but due to entropic considerations the average density will be observed. In this respect it is important to note that the estimate of the critical point by Panagiotopoulos, [2] $T_c^* = 1\cdot32$, is below the generally accepted value. $T_c^* = 1\cdot35$ [8]. However, the latter value is based on N,V,T-simulations of a finite systems. Hansen and Verlet [9] have shown that finite size effects lead to an overestimation of the critical temperature of the same order of magnitude. Unlike the conventional simulations the Gibbs ensemble allows for fluctuations in the volume as well as the number of particles. It seems that the Gibbs ensemble therefore leads to a better estimate of the critical temperature for the infinite system. It would therefore be interesting to investigate these aspects more carefully by applying finite size scaling techniques to the density probability functions [10].

Appendix 1

The free energy density for an ideal gas

For the ideal gas, the Gibbs partition function is given by

$$\bar{Z}_{N, V, T} = \frac{1}{\Lambda^{3N} N!} \sum_{N_1 = 0}^{N} \frac{N!}{N_1! N_2!} \int_0^V dV_1 V_1^{N_1} V_2^{N_2}$$

$$= NV \int_0^1 dx \int_0^1 dy \bar{Z}_N(x, y), \qquad (A\,1)$$

where

$$\bar{Z}_N(x, y) = \frac{V^N}{(xN)!((1 - x)N)!} y^{xN}(1 - y)^{(1 - x)N}. \qquad (A\,2)$$

Using Stirling's equation [11]

$$\ln n! = \left(n + \frac{1}{2}\right) \ln n - n + C^{\text{ste}} + o\left(\frac{1}{n}\right), \qquad (A\,3)$$

we can then write

$$Z_N(x, y) = \exp\left\{V\rho\left(x \ln\left(\frac{x}{y}\rho\right) + (1 - x)\ln\left(\frac{1 - x}{1 - y}\rho\right) - 1\right)\right.$$

$$\left. - \ln(\rho V) - \tfrac{1}{2}\ln(x(1 - x)) + 2C^{\text{ste}} + o\left(\frac{1}{V}\right)\right\}. \qquad (A\,4)$$

To determine the function $G(x, y)$, we look at the moments

$$\langle x^n y^m \rangle = \lim_{V \to \infty} \frac{\int_0^1 dx \int_0^1 dy x^n y^m \bar{Z}_N(x, y)}{\int_0^1 dx \int_0^1 dy \bar{Z}_N(x, y)}. \qquad (A\,5)$$

It is easy to verify that the surface S where $f(x, y)$ reaches its minimum is given by the points $x = y$. Therefore

$$\langle x^n y^m \rangle = \langle x^{n+m} \rangle. \qquad (A\,6)$$

Introducing u where $y = x(1 + u)$, we then change the integration variables to x, u. Since only small values of u contribute to the integral, we can expand in powers of u. Up to second order we find

$$\langle x^n y^m \rangle = \lim_{N \to \infty} \frac{\int_0^1 dx \int_{-1}^{(1/x) - 1} dux \frac{x^{n+m}}{\sqrt{[x(1 - x)]}} \exp\left[-\left(Nx + \frac{Nx^2}{(1 - x)}\right)\frac{u^2}{2}\right]}{\int_0^1 dx \int_{-1}^{(1/x) - 1} du \frac{x}{\sqrt{[x(1 - x)]}} \exp\left[-\left(Nx + \frac{Nx^2}{(1 - x)}\right)\frac{u^2}{2}\right]}. \qquad (A\,7)$$

The integration interval with respect to u can be replaced by $[-\infty, +\infty]$. We then find

$$\langle x^n y^m \rangle = \frac{\int_0^1 dx x^{n+m}}{\int_0^1 dx 1}, \qquad (A\,8)$$

which implies that

$$G(x, y) = \delta(x - y). \qquad (A\,9)$$

Appendix 2

Computation details of the presented simulations

In this Appendix a very short description of the computation details will be given. A more extensive description of the simulation techniques is provided in [2] and [3]. We have performed the simulations in cycles, each cycle having three steps: a displacement step, a change of the volume and attempts to change the number of particles.

In the displacement step all particles in box 1 successively are given a random displacement. The maximum displacement was chosen in such a way that the acceptance ratio was approximately 50 per cent. The same procedure was repeated for box 2.

The next step was an attempt to change the volume of box 1 by an amount ΔV and consequently the volume of box 2 changed by $-\Delta V$. The maximum volume change was adjusted to give an acceptance ratio of approximately 50 per cent. We have calculated the energy change associated with this volume change utilizing the scaling properties of the Lennard-Jones potential [12].

The final step of the cycle is N_{tr} attempts to insert a particle (usually we have taken N_{tr} as half the total number of particles). Before each attempt it is decided at random which box will receive a particle.

The Lennard-Jones potential was truncated at half the box size and the usual long tail corrections were applied. For each simulation we performed at least 2000 equilibrium cycles. The number of production cycles was at least 6000 and greater close to the critical temperature.

In [2] it is mentioned that close to the critical point some simulations failed because one of the boxes became empty. However, inspection of the partition function (equation (11)) shows that one must allow for $N_1 = 0$ (box one empty) and $N_1 = N$ (box two empty) in order to calculate ensemble averages correctly. So, it is important to ensure that the program does not fail because of technical reasons when one of the boxes becomes empty. For example, when one of the boxes is empty the addition of yet another particle to the full box may cause a division by zero. This addition will lead to a situation with $N + 1$ particles and inspection of the partion function (equation (11)) shows that this configuration should not be sampled. However, if one also calculates the chemical potential during the exchange step one should be careful. In order to calculate the chemical potential correctly [6] one should also add *test particles* when one of the boxes is full. Furthermore, when one of the boxes is empty it is (theoretically) possible that successive volume changes may lead to a negative volume of this box and this should be avoided in the same way.

References

[1] ALLEN, M. P., and TILDESLEY, D. J., 1987, *Computer Simulation of Liquids* (Clarendon).
[2] PANAGIOTOPOULOS, A. Z., 1987, *Molec. Phys.*, **61**, 813.
[3] PANAGIOTOPOULOS, A. Z., QUIRKE, N., STAPLETON, M., and TILDESLEY, D., 1988, *Molec. Phys.*, **63**, 527.
[4] RUELLE, D., 1969, *Statistical Mechanics, Rigorous results* (Benjamin).
[5] DINGLE, R. B., 1973, *Asymptotic Expansions, their Derivation and Interpretation* (Academic Press).
[6] FRENKEL, D., 1988, *Monte Carlo Simulations* (Proceedings of the NATO ASI on Computer Modelling of Fluids, Polymers and Solids), edited by C. R. A. Catlow. SMIT, B., and FRENKEL, D., 1989, *Molec. Phys.*, **68**, 951.

[7] ROWLINSON, J. S., and WIDOM, B., 1982, *Molecular Theory of Capillarity* (Clarendon).
[8] NICOLAS, J. J., GUBBINS, K. E., STREET, W. B., and TILDESLEY, D. J., 1979, *Molec. Phys.*, **37**, 1429.
[9] HANSENS, J. P., and VERLET, L., 1969, *Phys. Rev.*, **184**, 151.
[10] BINDER, K., 1981, *Z. Phys.* B, **43**, 119.
[11] ABRAMOWITZ, M., and STEGUN, I., 1970, *Handbook of Mathematical Functions* (Dover).
[12] McDONALD, I. R., 1972, *Molec. Phys.*, **23**, 41.